Journal of
Applied and Computational Mechanics

Shahid Chamran University of Ahvaz

Research Paper

An Exact Analytical Solution for Heat Conduction in a Functionally Graded Conical Shell

Amin Amiri Delouei[1], Amin Emamian[2], Sajjad Karimnejad[3], Yueming Li[4]

[1] Department of Mechanical Engineering, University of Bojnord, Bojnord 945 3155111, Iran, Email: a.amiri@ub.ac.ir

[2] Mechanical Engineering Department, Shahrood University of Technology, Shahrood, 361 9995161, Iran, Email: aminemamian70@mail.com

[3] Mechanical Engineering Department, Shahrood University of Technology, Shahrood, 361 9995161, Iran, Email: karimnejad.sajjad@gmail.com

[4] State Key Laboratory for Strength and Vibration of Mechanical Structures, Shaanxi Key Laboratory of Environment and Control for Flight Vehicle, School of Aerospace Engineering, Xi'an Jiaotong University, Xi'an, 710049, The People's Republic of China, Email: liyueming@xjtu.edu.cn

Abstract. In this study, an exact analytical solution for the heat conduction problem in a truncated conical shell is presented. The cone is made of functionally graded materials and it is considered that the material properties vary according to power-law functions. The general thermal boundary conditions are applied to cover a wide variety of actual applications. The results are successfully validated. Two examples, which are tried to mimic practical conditions, are studied using the derived solution, and a parametric study is done to shed light on the problem. The outcomes of this research provide useful information for understanding the nature of heat transfer behavior in the specific geometry of a cone. Regarding the specific applications of conical shells, the results can be used in the prefabrication process of these shells and tailoring the design parameter of functionally graded materials.

Keywords: Exact Analytical study, Conical shell, Functionally graded material, Heat conduction, General thermal boundary conditions.

1. Introduction

Functionally graded composite material has grown and also continued to grow in popularity due to its superior applications in biological fields, sports commodity and many others [1-8]. This is mainly resulted from their high durability, structural efficiency, better serviceability, and performance in harsh condition like exposure to high thermal and stress load [1, 9, 10]. Functionally graded material (FGM) is definitely considered as one of the most sophisticated and diverse classes of materials [11-14]. The rate of enhancement and study therefore accelerated in recent years, and it is shown that FGM has been used to remedy most problems seen during the utilization of other materials like conventional composites [15, 16]. Many structures are composites, particularly natural biological ones like tendon-to-bone insertion zone which are generally comprised of several different constituents [1, 11, 17]. Compared to traditional composite materials [18-24], FGMs are rather different. For one thing, FGM is a new and advanced generation of composite materials in which different materials are merged together continuously [25]. As a result, a non-homogeneous microstructure with continuously varied macro properties (like thermal conductivity and density) is obtained [25, 26].

Generally, FGMs are designed to handle and endure high temperature situation. Thus, studying them under complex and large temperature gradient is of great value [25, 27, 28]. To do so, a number of different methods such as numerical and analytical techniques have been utilized to conduct researches [29]. As for the former, one can refer to finite element method [30] as well as boundary element method [31]. In the case of materials with continuously varying property, finite element method is not efficient. boundary element method also requires treating singular and near-singular integrals which results in high computational costs [31]. However, the latter has shown promising results in the case of studying thermal characteristics of FGMs [2, 20, 21]. To benefit from the inherent merits of accurate results, many have utilized analytical methods to tackle various problems [2, 11, 32-34].

As for common geometries like tubes, plates [35], cylinders [36-41], and spheres [42] there are a number of studies concerning them. A thorough review on the different theoretical methods which are utilized for studying FGM shells and plates subjected to thermal and mechanical loading is done in Ref. [43]. A critical review on the different analytical and numerical methods utilized for analyzing heat inclusion in FGM plates is reported in [35] and it is tried to classify various solution methods. Lu et al. [33] presented an analytical method to acquire a closed-solution for temperature distribution in a cylinder. Hosseini et al. [44] studied the problem of heat transfer inside an axisymmetric cylindrical shells made of FGM by means of analytical methods. The material properties are assumed to be nonlinear and distributed with a power-law function through its thickness [44]. Dai et al. [36]

collated the research done on the cylindrical FGMs between 2005 and 2015. Amiri Delouei et al. [2] recently reported an analytical axisymmetric solution for heat conduction in a finite FG cylinder subjected to general boundary conditions. Also, two exact analytical solutions for heat conduction in FG cylindrical segments [34] and FG spherical shells [35] under general thermal boundary conditions are presented. Eslami et al. [45] studied the behavior of a spherical shell made of FGM when temperature distribution is solely a function of radius. Unlike above-mentioned outlines, for complex shells such as cones, literature is very narrow [46, 47]. However, due to the numerous applications of these types of shells, thermal investigation of them seems necessary. Some studies in this regard were restricted to mechanical buckling and free vibration [48-50].

FGMs superior benefits, particularly for thermal loading, mainly stem from the fact that for various uses one can tailor them and customize their response especially for harsh thermal environment. As a result of which, the knowledge over the performance of FGM and the prediction of its behavior is of great importance. Authors in this study, therefore, aimed at studying the problem of two-dimensional (2D) heat conduction in a truncated conical shell made of FGM which is subjected to general thermal boundary conditions. Unfortunately, despite the widespread use of this geometry in various commercial industries, little research has been done in this area. The analytical approach is employed to obtain the most accurate results. Two illustrative case examples are also investigated to check the capability of the obtained analytical solution.

2. Mathematical approach

In the current study, the steady-state heat conduction in a conical shell made of FGM is investigated. Fig. 1 shows the coordinate system of the present geometry. Accordingly, y is in the direction of coincident on the straight line that links apex point of cone to its base. ϕ is parallel with the base plane in the tangent direction in the lateral surface.

It is worth mentioning that 2D heat transfer in FG structures can be orthotropic, so conduction tensor for such materials is diagonal in which there is only k_y and k_ϕ [51, 52]. Applying the balance of energy on the element presented by Fig. 1, the subsequent relation will be obtained:

$$\frac{\partial\left(k_y\frac{\partial T}{\partial y}\varepsilon Rd\phi\right)}{\partial y}dy + \frac{\partial\left(k_\phi\frac{\partial T}{R\partial\phi}\varepsilon dy\right)}{\partial y}d\phi - h\left(T - T_{r,\infty}\right)dyRd\phi = \rho c\frac{\partial T}{\partial t}dV \, , \tag{1}$$

here T, c and ρ respectively indicate the temperature distribution, heat capacity and density. The thickness of the shell is identified with ε. The parameter of R (radius of cone's annular cross section) is shown in Fig. 2. k_y, k_ϕ are the heat conductivity in y and ϕ directions, respectively. Also, and $T_{r,\infty}$ is the ambient temperature. It is presumed that the thermal conductivity, k_y, is the power functions of y as [53]:

$$k_y = k_1 y^{-\alpha} \, , \tag{2}$$

k_ϕ is equal to k_2, k_ϕ, k_1, k_2 and α are the material constants for the ceramic material and β is the ratio of k_1 to k_2. Further, α is considered to express the inhomogeneity of the structure [51, 53].

Because of the small thickness of the cone, the lump condition is considered in thickness direction. Eq. 3 is binding between R and y:

$$R = y\sin\varphi \, . \tag{3}$$

$$\frac{\partial\left(k_y\frac{\partial T}{\partial y}\epsilon Rd\phi\right)}{\partial y}dy + \frac{\partial\left(k_\phi\frac{\partial T}{R\,\partial\phi}\epsilon dy\right)}{\partial\phi}d\phi - h(T-T_{r,\infty})dyRd\phi = \rho c\frac{\partial T}{\partial t}dV$$
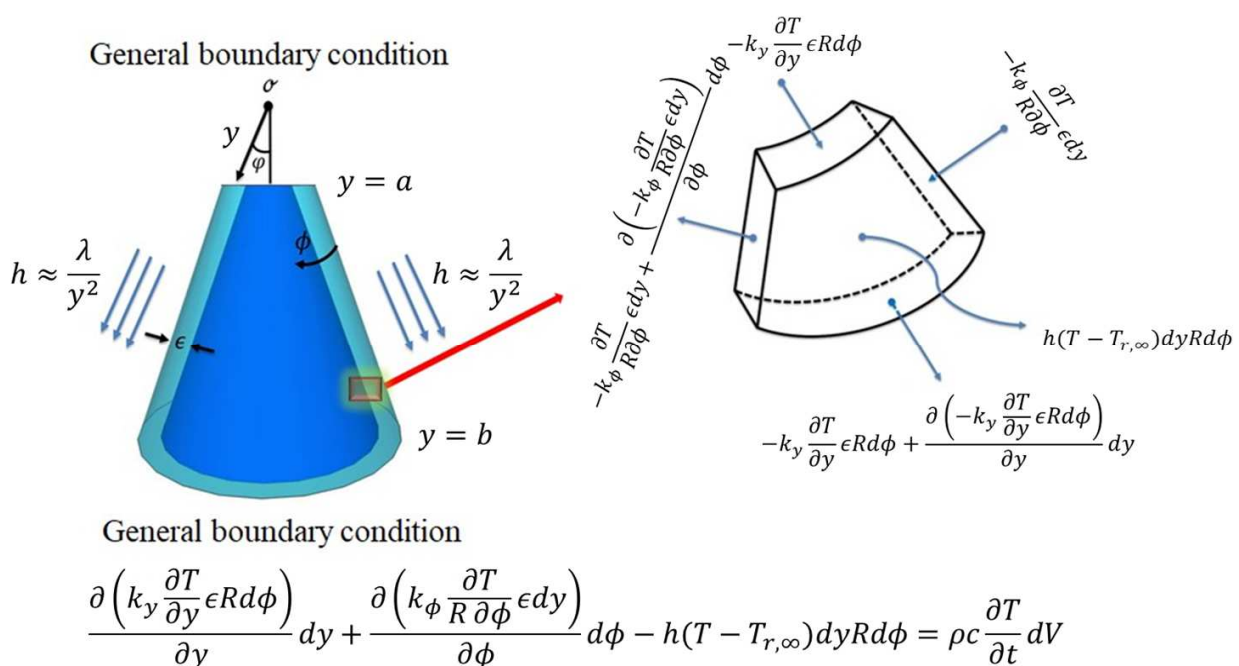
Fig. 1. Schematic illustration of the problem

In practice, coefficient of heat conduction is not a constant value and generally depends on the outline of the body and flow around it. In the case of a cone, following relation is used to describe this coefficient around the shell [54, 55]:

$$h \approx \frac{\lambda}{y^2} \,, \tag{4}$$

where λ is a constant, and h is the heat convection coefficient. By substituting Eq. (4) into Eq. (1), the following equation is achieved for heat transfer conduction of conical shell:

$$\frac{\partial\left(k_y \dfrac{\partial T}{\partial y}\epsilon R d\phi\right)}{\partial y}dy + \frac{\partial\left(k_\phi \dfrac{\partial T}{R\partial\phi}\epsilon dy\right)}{\partial\phi}d\phi - \frac{\lambda}{y^2}(T - T_{r,\infty})dyRd\phi = \rho c\frac{\partial T}{\partial t}dV \,. \tag{5}$$

By considering the following modified temperature

$$\Theta(y,\phi) = T(y,\phi) - T_{r,\infty} \,. \tag{6}$$

Steady-state conduction in the axisymmetric condition is expressed as:

$$\frac{\partial}{\partial y}\left(yk_y\frac{\partial\Theta}{\partial y}\right) + \frac{1}{y\sin^2\varphi}\frac{\partial}{\partial\phi}\left(k_\phi\frac{\partial\Theta}{\partial\phi}\right) - \frac{\lambda}{\epsilon y}\Theta = 0 \,, \tag{7}$$

or

$$yk_y\frac{\partial^2\Theta}{\partial y^2} + k_y\frac{\partial\Theta}{\partial y} + \frac{\partial k_y}{\partial y}y\frac{\partial\Theta}{\partial y} + \frac{1}{y\sin^2\varphi}\frac{\partial}{\partial\phi}\left(k_\phi\frac{\partial\Theta}{\partial\phi}\right) - \frac{\lambda}{\epsilon y}\Theta = 0 \,. \tag{8}$$

The exploited general linear boundary conditions are as follows:

$$\mu\Theta(y,\phi) + \upsilon\frac{\partial\Theta(y,\phi)}{\partial y} = w_1(\phi) \quad y = a \,, \tag{9}$$

$$\delta\Theta(y,\phi) + \varepsilon\frac{\partial\Theta(y,\phi)}{\partial y} = w_2(\phi) \quad y = b \,. \tag{10}$$

$w_1(\phi)$ and $w_2(\phi)$ are known as the arbitrary functions. The constants δ and μ take the similar dimension as the coefficient of convection, and the constants ε and ν take the similar dimension as the coefficient of conduction.

3. Analytical solution

The following equation is obtained by introducing Eq. (2) into Eq. (8):

$$\beta y^{-\alpha}\left(y\frac{\partial^2\Theta(y,\phi)}{\partial y^2} + \frac{\partial\Theta(y,\phi)}{\partial y}(-\alpha + 1)\right) - \frac{\lambda}{k_2\epsilon y}\Theta(y,\phi) + \frac{1}{y\sin^2\varphi}\frac{\partial^2\Theta(y,\phi)}{\partial\phi^2} = 0 \,, \tag{11}$$

Two independent functions can be used to define the temperature distribution:

$$\Theta(y,\phi) = \Lambda(y)\Gamma(\phi) \,, \tag{12}$$

Introducing Eq. (12) to Eq. (11):

$$\sin^2\varphi\left(\beta y^{-\alpha}\left(y^2\frac{\Lambda''(y)}{\Lambda(y)} + y(-\alpha + 1)\frac{\Lambda'(y)}{\Lambda(y)}\right) - \frac{\lambda}{k_2\epsilon}\right) = -\frac{\Gamma''(\phi)}{\Gamma(\phi)} = \Delta^2 \,, \tag{13}$$

where Δ is a constant and considered to be an eigenvalue for heat transfer equation. Applying the separation of variables (SOV) technique to solve Eq. (11) and applying homogeneous boundary conditions, the following equations in the ϕ direction are obtained:

$$\Gamma''(\phi) + \Delta^2\Gamma(\phi) = 0 \,, \tag{14}$$

$$\Gamma(0) = \Gamma(2\pi) \,, \tag{15}$$

$$\frac{\partial\Gamma(0)}{\partial\phi} = \frac{\partial\Gamma(2\pi)}{\partial\phi} \,. \tag{16}$$

General answer for Eq. (14) is as:

$$\Gamma(\phi) = a_n\cos(\Delta_n\phi) + b_n\sin(\Delta_n\phi) \,, \tag{17}$$

Substituting Eq. (17) on boundary conditions (Eqs. (15) and (16)), the following equations are found:

$$a_n\left(\cos(2\pi\Delta_n) - 1\right) + b_n\sin(2\pi\Delta_n) = 0 \,, \tag{18a}$$

$$a_n \sin(2\pi\Delta_n) - b_n\left(\cos(2\pi\Delta_n) - 1\right) = 0 \ . \tag{18b}$$

As known, these equations are homogeneous. Consequently, related answers are zero unless they are linear dependent. In other words, if the determinant of coefficients in Eqs. (18) is zero then answers are available.

$$\left(\cos(2\pi\Delta_n) - 1\right)^2 + \sin^2(2\pi\Delta_n) = 0 \ . \tag{19}$$

By solving trigonometric Eq. (19), eigenvalues will be achieved:

$$\Delta_n = n \qquad\qquad n = 0,1,2,\dots \ . \tag{20}$$

The following relations are resulted from Eq. (13) and corresponding boundary conditions in the y direction (Eqs. (9) and (10)):

$$\sin^2\varphi\left(\beta y^{-\alpha}\left(y^2\Lambda''(y) + y(-\alpha + 1)\Lambda'(y)\right) - \left(\frac{\lambda}{k_2\epsilon} + \frac{\Delta}{\sin^2\varphi}\right)\Lambda(y)\right) = 0 \ , \tag{21}$$

The general solution of this equation will be as:

$$\Lambda(y) = \begin{cases} y^{\frac{\alpha}{2}}\left(A_0 I_1\left(\zeta_0 y^{\frac{\alpha}{2}}\right) + B_0 K_1\left(\zeta_0 y^{\frac{\alpha}{2}}\right)\right) & n = 0 \\[2mm] y^{\frac{\alpha}{2}}\left(c_n I_1\left(\zeta y^{\frac{\alpha}{2}}\right) + d_n K_1\left(\zeta y^{\frac{\alpha}{2}}\right)\right) & n \geq 1 \end{cases} \ , \tag{22a}$$

where

$$\zeta = -\frac{2}{\alpha}\sqrt{\frac{\lambda\sin^2\varphi + \Delta_n^2 k_2\epsilon}{k_1\epsilon\sin^2\varphi}}, \quad \zeta_0 = -\frac{2}{\alpha}\sqrt{\frac{\lambda}{k_1\epsilon}} \ , \tag{22b}$$

The temperature distribution is achieved by the product of independent functions:

$$\Theta(y,\phi) = y^{\frac{\alpha}{2}}\left(A_0 I_1\left(\zeta_0 y^{\frac{\alpha}{2}}\right) + B_0 K_1\left(\zeta_0 y^{\frac{\alpha}{2}}\right)\right) + \sum_{n=1}^{\infty} y^{\frac{\alpha}{2}}\left(A_n I_1\left(\zeta y^{\frac{\alpha}{2}}\right) + B_n K_1\left(\zeta y^{\frac{\alpha}{2}}\right)\right)\cos(\Delta_n\phi) + \sum_{n=1}^{\infty} y^{\frac{\alpha}{2}}\left(C_n I_1\left(\zeta y^{\frac{\alpha}{2}}\right) + D_n K_1\left(\zeta y^{\frac{\alpha}{2}}\right)\right)\sin(\Delta_n\phi) \ , \tag{23}$$

Lastly, by introducing the inner and outer boundary conditions in y direction, the unknown coefficients will be achieved. Introducing the temperature distribution of Eq. (23) into equations of 9 and 10, the following equations will be obtained:

$$A_0 M_0 + B_0 N_0 + \sum_{n=1}^{\infty}\left(A_n M_n + B_n N_n\right)\cos(\Delta_n\phi) + \sum_{n=1}^{\infty}\left(C_n M_n + D_n N_n\right)\sin(\Delta_n\phi) = w_1(\phi) \ , \tag{24a}$$

$$A_0 P_0 + B_0 Q_0 + \sum_{n=1}^{\infty}\left(A_n P_n + B_n Q_n\right)\cos(\Delta_n\phi) + \sum_{n=1}^{\infty}\left(C_n P_n + D_n Q_n\right)\sin(\Delta_n\phi) = w_2(\phi) \ , \tag{24b}$$

where

$$M_0 = \mu a^{\frac{\alpha}{2}} I_1\left(\zeta_0 a^{\frac{\alpha}{2}}\right) + \upsilon\frac{\alpha\zeta_0 a^{\alpha-1}}{2} I_0\left(\zeta_0 a^{\frac{\alpha}{2}}\right) \ , \tag{25a}$$

$$N_0 = \mu a^{\frac{\alpha}{2}} K_1\left(\zeta_0 a^{\frac{\alpha}{2}}\right) + \upsilon\frac{\alpha\zeta_0 a^{\alpha-1}}{2} K_0\left(\zeta_0 a^{\frac{\alpha}{2}}\right) \ , \tag{25b}$$

$$P_0 = \delta b^{\frac{\alpha}{2}} I_1\left(\zeta_0 b^{\frac{\alpha}{2}}\right) + \varepsilon\frac{\alpha\zeta_0 b^{\alpha-1}}{2} I_0\left(\zeta_0 b^{\frac{\alpha}{2}}\right) \ , \tag{25c}$$

$$Q_0 = \delta b^{\frac{\alpha}{2}} K_1\left(\zeta_0 b^{\frac{\alpha}{2}}\right) + \varepsilon\frac{\alpha\zeta_0 b^{\alpha-1}}{2} K_0\left(\zeta_0 b^{\frac{\alpha}{2}}\right) \ . \tag{25d}$$

and

$$M_n = \mu a^{\frac{\alpha}{2}} I_1\left(\zeta a^{\frac{\alpha}{2}}\right) + \upsilon\frac{\alpha\zeta a^{\alpha-1}}{2} I_0\left(\zeta a^{\frac{\alpha}{2}}\right) \ , \tag{26a}$$

$$N_n = \mu a^{\frac{\alpha}{2}} K_1\left(\zeta a^{\frac{\alpha}{2}}\right) + \upsilon\frac{\alpha\zeta a^{\alpha-1}}{2} K_0\left(\zeta a^{\frac{\alpha}{2}}\right) \ , \tag{26b}$$

$$P_n = \delta\, b^{\frac{\alpha}{2}} I_1\left(\zeta b^{\frac{\alpha}{2}}\right) + \varepsilon\, \frac{\alpha \zeta b^{\alpha-1}}{2} I_0\left(\zeta b^{\frac{\alpha}{2}}\right), \tag{26c}$$

$$Q_n = \delta\, b^{\frac{\alpha}{2}} K_1\left(\zeta b^{\frac{\alpha}{2}}\right) + \varepsilon\, \frac{\alpha \zeta b^{\alpha-1}}{2} K_0\left(\zeta b^{\frac{\alpha}{2}}\right). \tag{26d}$$

In continue, the following equations via the existing relations for orthogonal functions will be constructed:

$$A_0 M_0 + B_0 N_0 = F_{0,i}, \tag{27a}$$

$$A_0 P_0 + B_0 Q_0 = F_{0,i}, \tag{27b}$$

$$A_n M_n + B_n N_n = F_{\cos,i}, \tag{27c}$$

$$A_n P_n + B_n Q_n = F_{\cos,i}, \tag{27d}$$

$$C_n M_n + D_n N_n = F_{\sin,i}, \tag{27e}$$

$$C_n P_n + D_n Q_n = F_{\sin,i}, \tag{27f}$$

where

$$F_{0,i} = \frac{1}{2\pi} \int_0^{2\pi} w_i(\phi)\, d\phi, \qquad i = 1,2, \tag{28a}$$

$$F_{\cos,i} = \frac{1}{\pi} \int_0^{2\pi} w_i(\phi) \cos(\Delta_n \phi)\, d\phi, \qquad i = 1,2, \tag{28b}$$

$$F_{\sin,i} = \frac{1}{\pi} \int_0^{2\pi} w_i(\phi) \sin(\Delta_n \phi)\, d\phi, \qquad i = 1,2. \tag{28c}$$

The unknown coefficients of A_n, B_n, C_n and D_n can be achieved as follows:

$$A_0 = -\frac{F_{0,1} Q_0 - F_{0,2} N_0}{P_0 N_0 - M_0 Q_0}, \tag{29a}$$

$$B_0 = \frac{F_{0,1} P_0 - F_{0,2} M_0}{P_0 N_0 - M_0 Q_0}, \tag{29b}$$

$$A_n = -\frac{F_{\cos,1} Q_n - F_{\cos,2} N_n}{P_n N_n - M_n Q_n}, \tag{29c}$$

$$B_n = \frac{F_{\cos,1} P_n - F_{\cos,2} M_n}{P_n N_n - M_n Q_n}, \tag{29d}$$

$$C_n = -\frac{F_{\sin,1} Q_n - F_{\sin,2} N_n}{P_n N_n - M_n Q_n}, \tag{29e}$$

$$D_n = \frac{F_{\sin,1} P_n - F_{\sin,2} M_n}{P_n N_n - M_n Q_n}, \tag{29f}$$

4. Results and discussion

The solution developed in the previous section is now hired here to assess the temperature distribution for two illustrative cases. It is tried to capture the practical conditions. Parameters used for the two aforementioned cases are shown in Table 1. The schematic illustrations of two cases along with applied thermal boundary conditions for case 1 and 2 are plotted in Fig. 2 and 3, respectively.

Table 1. Parameters used for the two aforementioned cases

	Parameter	Case 1	Case 2
1	φ	$\pi/9$	$\pi/9$
2	$\epsilon\ [m]$	0.01	0.01
3	$a\ [m]$	0.1	0.1
4	$b\ [m]$	1	1
5	$\delta\ [W/m^2K]$	10	10
6	$T_{y,\infty}\ [K]$	200	250

4.1. Verification test

Before proceeding, the credibility of the obtained solution is checked against acquired numerical results. Finite element method (FEM) is used to numerically solve the problem. In order to assess mesh independence, four various grid numbers, namely 56400, 98900, 134800, and 278600, are used. Out of many, 134800 elements is chosen to satisfy the computational accuracy and avoid computational costs.

Both first and second cases are tested and $\eta = 1357\ W/m^2$, $\beta = 1$, $\lambda = 2\ W/K$ are selected for the simulation purpose. Temperature distribution for two different values of α (2 and 3) in y direction is considered. As can be seen from Fig. 4 a and b, there is a good match among the results which shows the solution is capable of adequately predicting the distribution of temperature.
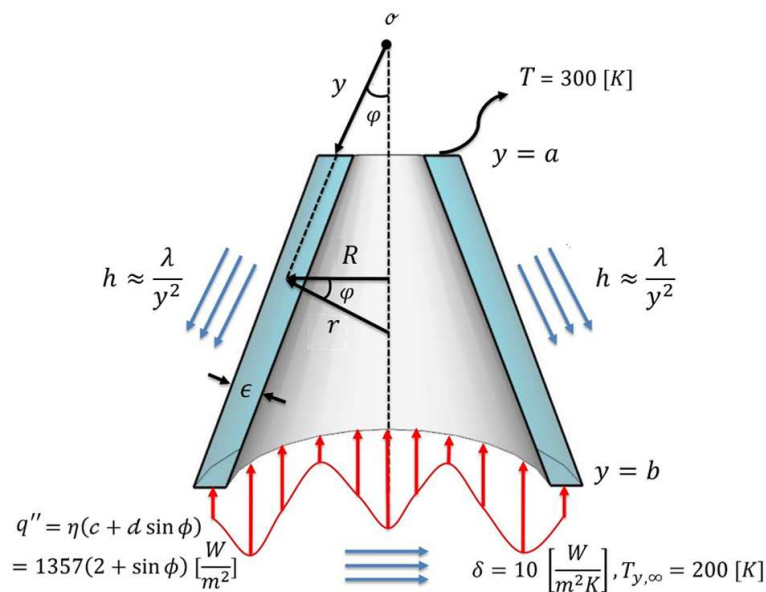
Fig. 2. Geometry and thermal boundary conditions of case 1
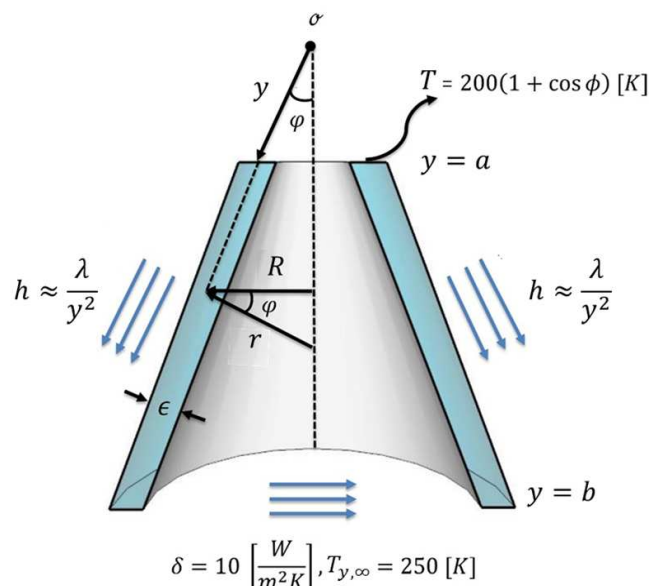
Fig. 3. Geometry and thermal boundary conditions of case 2
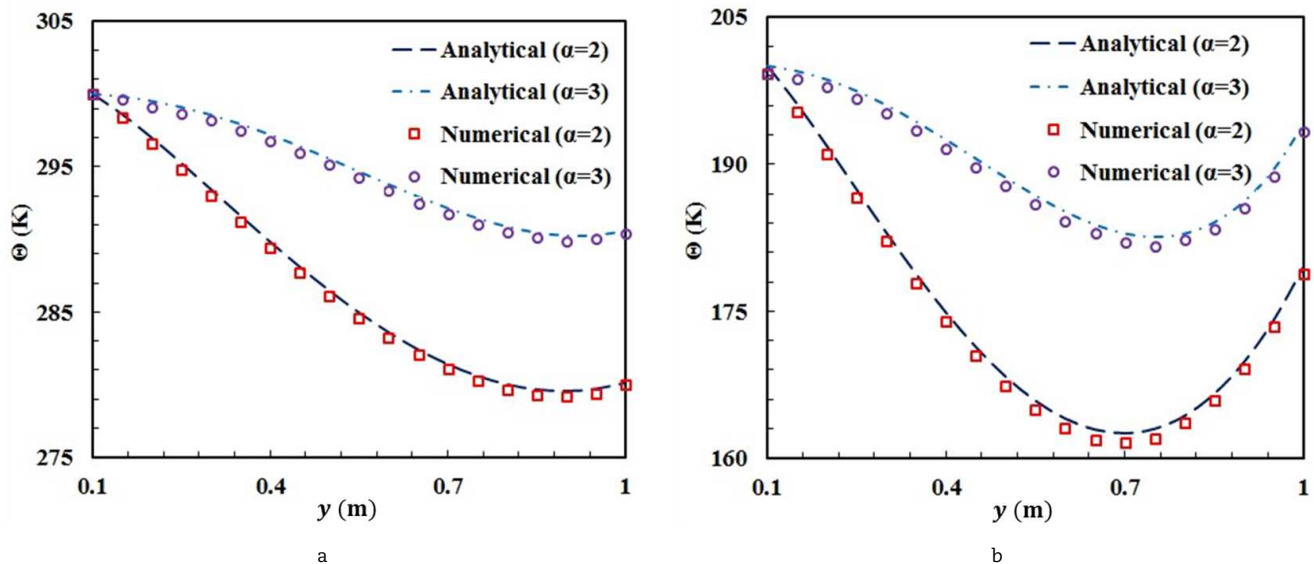
Fig. 4. Comparison of temperature distribution via numerical and analytical approaches in y direction for $\eta = 1357 \ W \ / \ m^2$, $\beta = 1$, $\lambda = 2 \ W \ / \ K$, and four values of α for a) case 1 and b) case 2
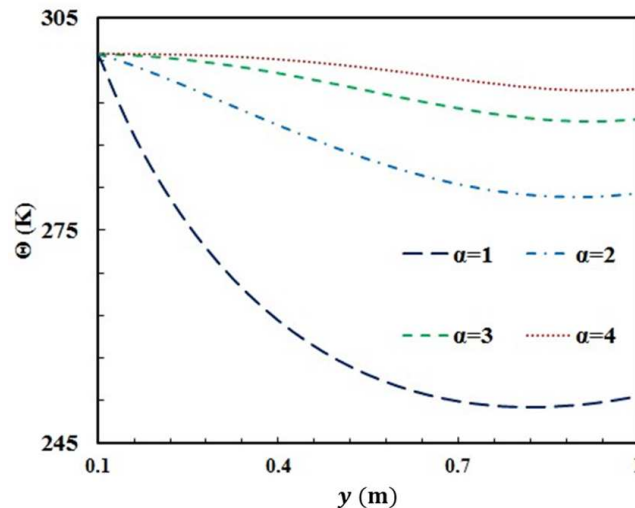

Fig. 5. Temperature distribution in y direction at $\eta = 1357 \ W \ / \ m^2$, $\beta = 1$, $\lambda = 2 \ W \ / \ K$ and (a) $\alpha = 1$, (b) $\alpha = 2$, (c) $\alpha = 3$, (d) $\alpha = 4$ for case 1.

4.2. Parametric study

4.2.1. Case one

As for the case 1 (Fig. 2 and Table. 1), the impact of different parameters like α, η, β and λ on the distribution of temperature in y and ϕ directions are investigated. As for the boundary conditions, w_1 and w_2 are considered to be 300 K and $\eta(2 + \sin \phi) + \delta T_{y,\infty}$, respectively. Figure 5 shows temperature distribution in y direction at $\eta = 1357 \ W \ / \ m^2$, $\beta = 1$, $\lambda = 2 \ W \ / \ K$ for four different values of α ranging from 1 to 4. Figure 6 also further reveals its impact using contours of temperature distribution in both y and ϕ directions. As can be seen, there is a wide disparity between that of α when equals 1 compared to other values. As it increases, the difference decreases and it is also seen that for $\alpha = 4$, the structure maintains almost the same level throughout the span.

The impact of η is presented by Figs. 7 and 8 which respectively indicate the profiles and contours of temperature distribution in y direction at $\alpha = 2$, $\beta = 1$, $\lambda = 2 \ W \ / \ K$ for different values of η (340, 680, 1010, 1357 W/m²). As expected, with an increase in the values of η, temperature will enhance. It is also seen that it leads to a state where structure tries to reach a plateau at the end.

Figures 9-12 are responsible for the influence of β and λ. Temperature distribution in y direction at $\alpha = 1$, $\eta = 1357 \ W \ / \ m^2$, $\lambda = 2 \ W \ / \ K$ for $\beta = 0.8$, 0.9, 1, and 1.1 along with its contours of temperature distribution (in both y and ϕ directions) are displayed in Figs. 9 and 10, respectively. As noted above, β is defined as the ratio of k_1 to k_2. From figures one can deduce that there is an equal difference among the figure for various values of conductivity ratio, and also all the lines show almost the same behavior. For instance, for $\beta = 0.8$ after hitting a low of about 244.3 K, the temperature distribution starts reversing its manner and it increases gradually.
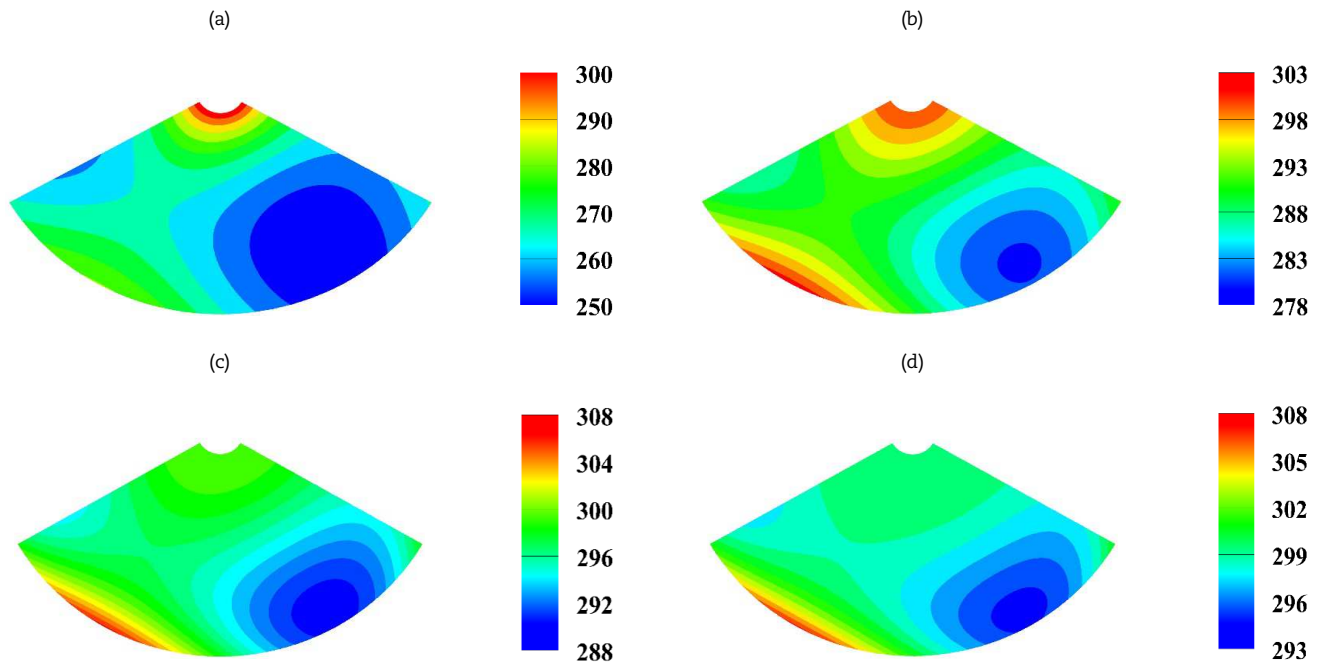
Fig. 6. Temperature (K) distribution contours in y and ϕ directions at $\eta = 1357\ W/m^2$, $\beta = 1$, $\lambda = 2\ W/K$ and (a) $\alpha = 1$, (b) $\alpha = 2$, (c) $\alpha = 3$, (d) $\alpha = 4$ for case 1.

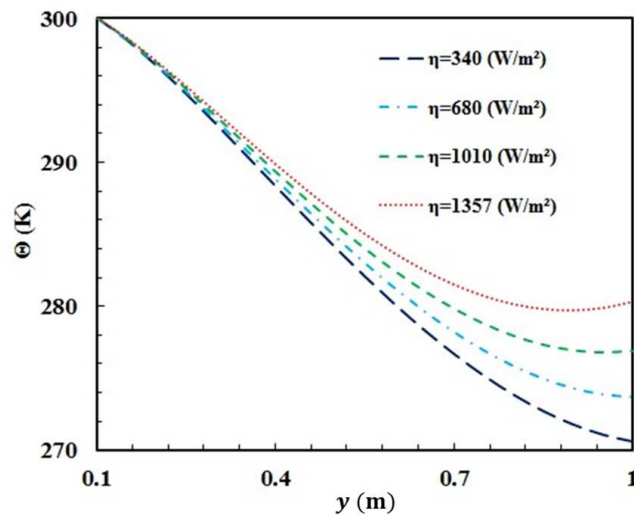**Fig. 7.** Temperature distribution in y direction at $\alpha = 2$, $\beta = 1$, $\lambda = 2\ W/K$ and (a) $\eta = 340\ W/m^2$, (b) $\eta = 680\ W/m^2$, (c) $\eta = 1010\ W/m^2$, (d) $\eta = 1357\ W/m^2$ for case 1.
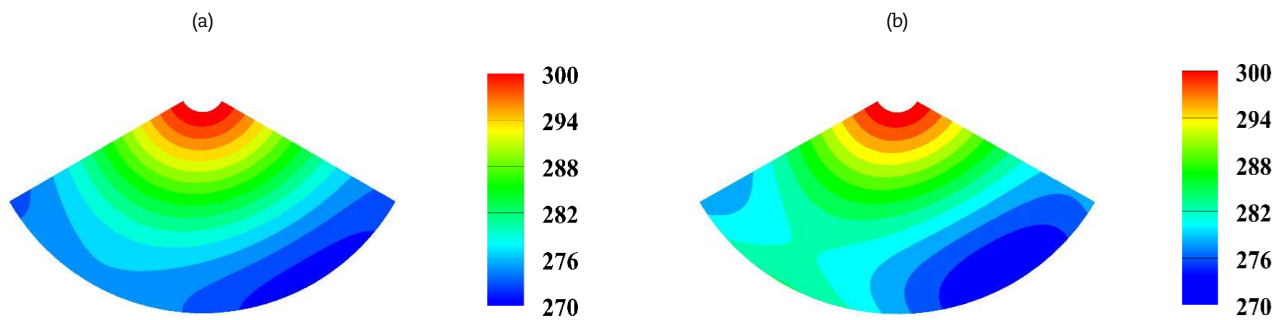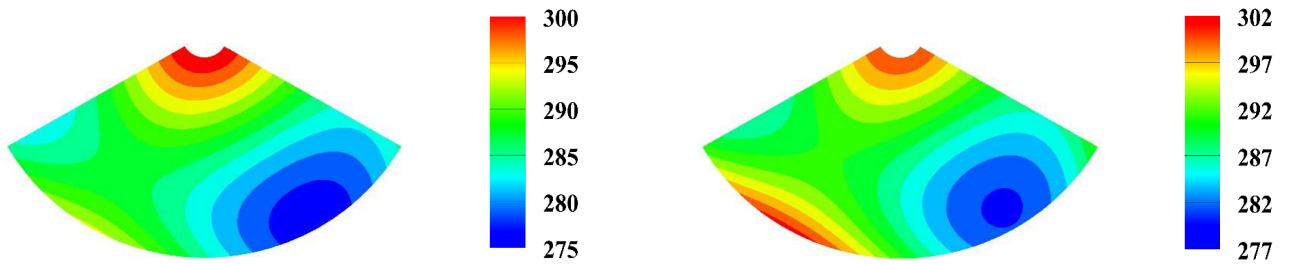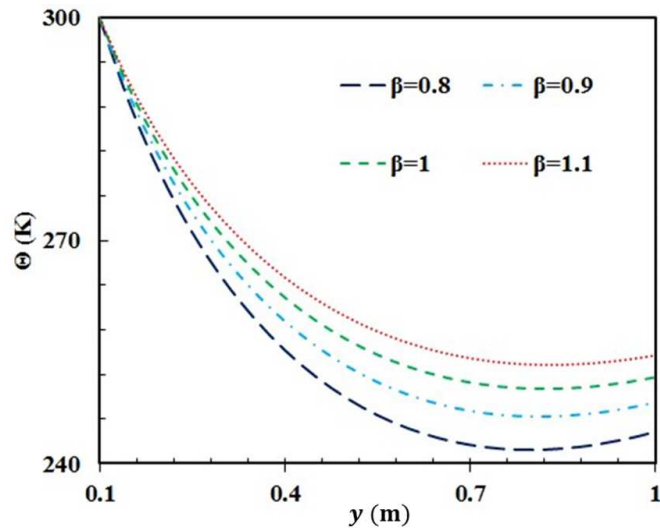

Fig. 8. Temperature (K) distribution contours in y and ϕ directions at $\alpha = 2$, $\beta = 1$, $\lambda = 2\ W/K$ and (a) $\eta = 340\ W/m^2$, (b) $\eta = 680\ W/m^2$, (c) $\eta = 1010\ W/m^2$, (d) $\eta = 1357\ W/m^2$ for case 1.

Fig. 8. Temperature (K) distribution contours in y and ϕ directions at $\alpha = 2$, $\beta = 1$, $\lambda = 2$ W / K and (a) $\eta = 340$ W / m^2 , (b) $\eta = 680$ W / m^2 , (c) $\eta = 1010$ W / m^2 , (d) $\eta = 1357$ W / m^2 for case 1.

Fig. 9. Temperature distribution in y direction at $\alpha = 1$, $\eta = 1357$ W / m^2, $\lambda = 2$ W / K and (a) $\beta = 0.8$, (b) $\beta = 0.9$, (c) $\beta = 1$, (d) $\beta = 1.1$ for case 1.
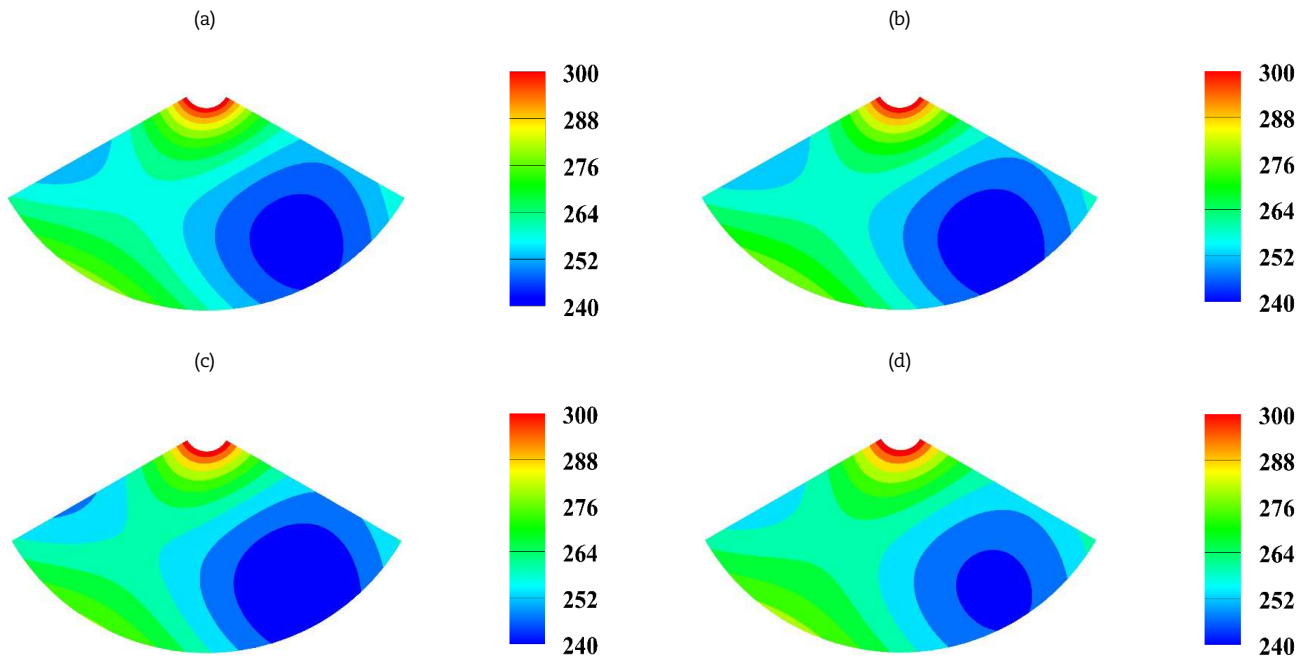
(a)   (b)

(c)   (d)

Fig. 10. Temperature (K) distribution contours in y and ϕ directions at $\alpha = 1$, $\eta = 1357$ W / m^2, $\lambda = 2$ W / K and (a) $\beta = 0.8$, (b) $\beta = 0.9$, (c) $\beta = 1$, (d) $\beta = 1.1$ for case 1.

On the other hand, from Figs. 11 and 12, the impact of λ on structure's thermal behavior can be seen. Specifically,

temperature distribution in y and ϕ directions at $\alpha = 2$, $\eta = 1357\ W/m^2$, $\beta = 1$ and for four values of λ (1, 2, 3, and 4 W/K) is assessed. As in figures, there is a rather considerable difference among the obtained results for different values of λ. While in the case of $\lambda = 4$ W/K, the structure keeps the same value throughout y direction, for other values of that (1, 2, and 3 W/K) temperature drops. This puts emphasis on the importance of the convection current around the body.

4.2.2. Case two

In the second case (Fig. 3 and Table. 1), like the previous section, the effect of some parameters including α, β, δ and λ are considered to investigate temperature distribution. As for the boundary conditions, w_1 and w_2 are considered to be $200(1 + \cos\phi)$ and $\delta\ T_{y,\infty}$, respectively. Temperature distribution in y and ϕ directions at $\delta = 10\ W/m^2K$, $\beta = 1$, $\lambda = 2\ W/K$ and different values of material constant ranging from 1 to 4 is investigated via Figs. 13 and 14. It can be seen that an increase in the value of material constant which defines material inhomogeneity will elevate thermal behavior of the cone. It also can be found out that for the lowest considered value of α, temperature distribution after reaching a minimum (almost 120 K) enhances rather significantly. As for the other values of α, the minimum values increase.
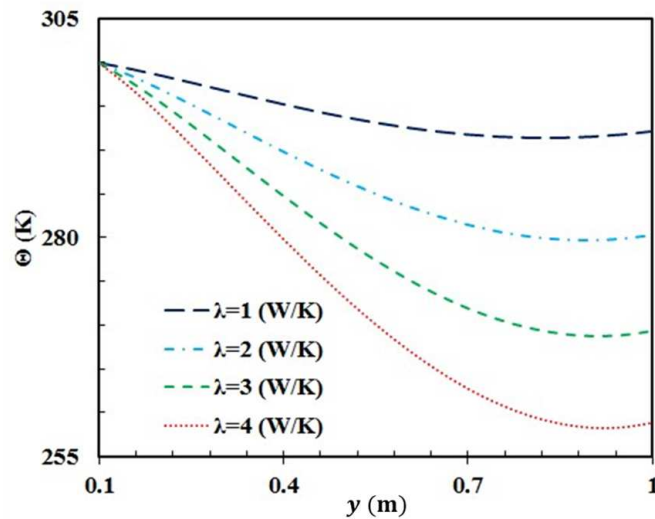

Fig. 11. Temperature distribution in y direction at $\alpha = 2$, $\eta = 1357\ W/m^2$, $\beta = 1$ and (a) $\lambda = 1\ W/K$, (b) $\lambda = 2\ W/K$, (c) $\lambda = 3\ W/K$, (d) $\lambda = 4\ W/K$ for case 1.
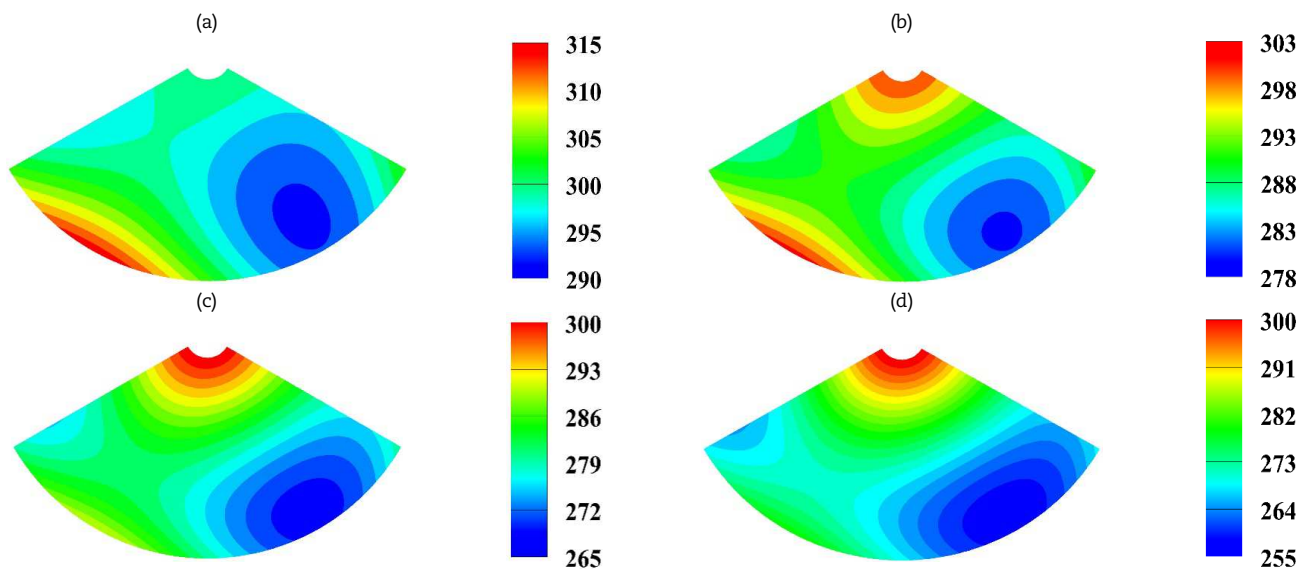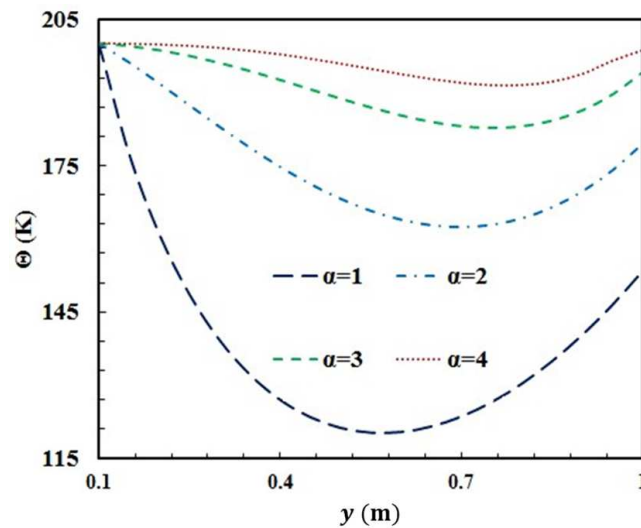

Fig. 12. Temperature (K) distribution contours in y and ϕ directions at $\alpha = 2$, $\eta = 1357\ W/m^2$, $\beta = 1$ and (a) $\lambda = 1\ W/K$, (b) $\lambda = 2\ W/K$, (c) $\lambda = 3\ W/K$, (d) $\lambda = 4\ W/K$ for case1.

Fig. 13. Temperature distribution in y direction at $\delta = 10\ W / m^2 K$, $\beta = 1$, $\lambda = 2\ W / K$ and (a) $\alpha = 1$, (b) $\alpha = 2$, (c) $\alpha = 3$, (d) $\alpha = 4$ for case 2.
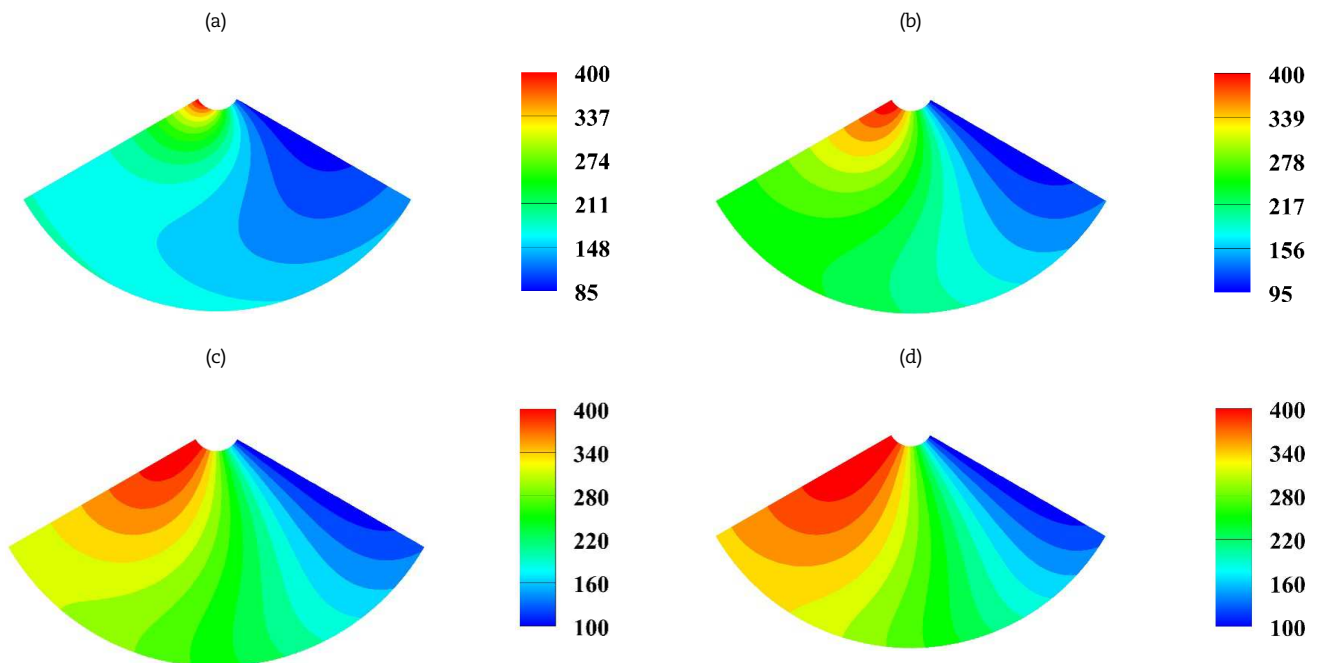

Fig. 14. Temperature (K) distribution contours in y and ϕ directions at $\delta = 10\ W / m^2 K$, $\beta = 1$, $\lambda = 2\ W / K$ and (a) $\alpha = 1$, (b) $\alpha = 2$, (c) $\alpha = 3$, (d) $\alpha = 4$ for case 2.

To further analyze, the effect of δ on the temperature distribution is also examined at $\alpha = 1$, $\beta = 1$, $\lambda = 2\ W / K$ in both y and ϕ directions (Figs. 15 and 16). It is seen that there is no significant difference in the figure for temperature between different values of δ until $y = 0.25m$. After which, the difference between them enhances. All the lines show somewhat the same manner. This can be seen from the contours of temperature distribution which is plotted in Fig. 16.

In addition, in both aforementioned directions, temperature distribution on the cone for different values of β at $\alpha = 1$, $\delta = 10\ W / m^2 K$, $\lambda = 3\ W / K$ as well as its corresponding contours is demonstrated in Figs. 17 and 18. At first, the quantity of temperature for the highest considered value, $\beta = 1$, was higher than other values. Afterwards, it was outstripped by $\beta = 0.1$, and then the other values. Further, it is seen that the quantity of the temperature for $\beta = 0.1$ after reaching the low of about 12 K at $y = 0.4m$, rises significantly so reaches its primary value.

Last but not least, temperature distribution at $\alpha = 1$, $\delta = 10\ W / m^2 K$, $\beta = 1$ in both y and ϕ directions for various values of λ are discussed through Figs. 19 and 20. With an increase in the values of λ from 1 to 4, temperature as well as the difference among the lines reduces.
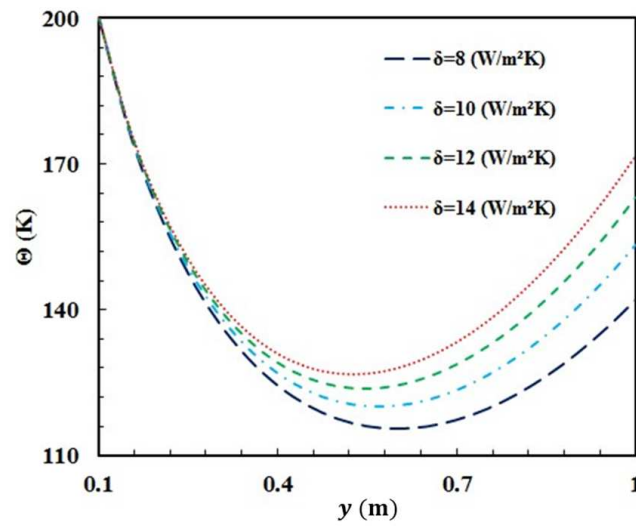
Fig. 15. Temperature distribution in y direction at $\alpha = 1$, $\beta = 1$, $\lambda = 2\,W\,/\,K$ and (a) $\delta = 8\,W\,/\,m^2K$, (b) $\delta = 10\,W\,/\,m^2K$, (c) $\delta = 12\,W\,/\,m^2K$, (d) $\delta = 14\,W\,/\,m^2K$ for case 2.
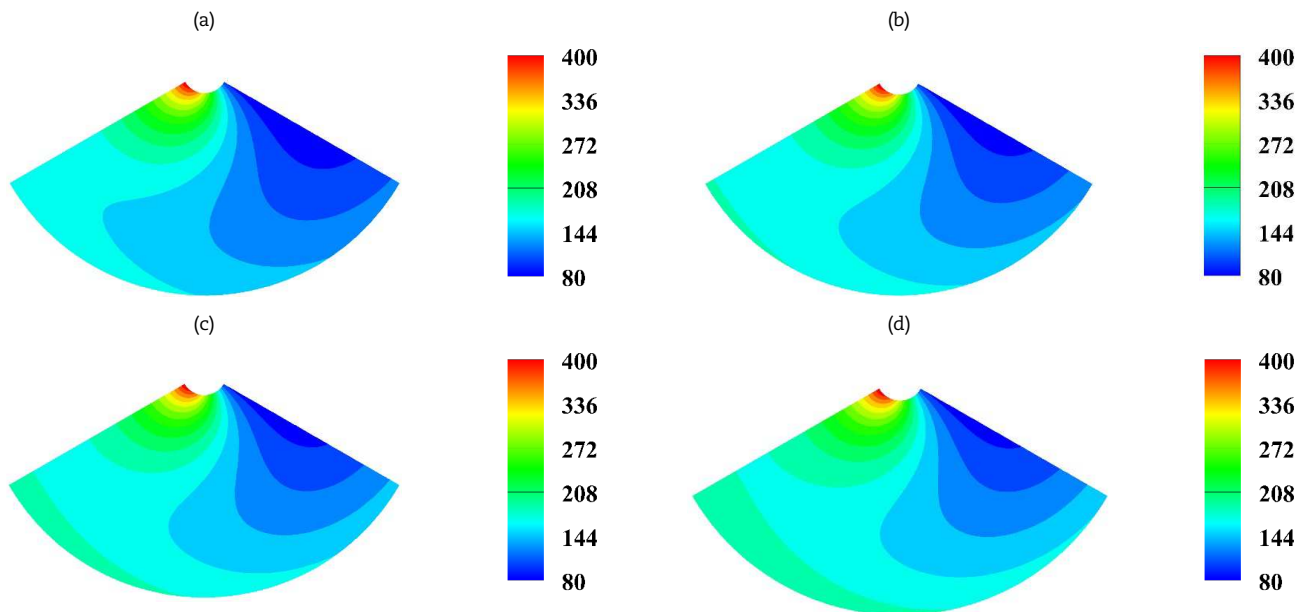

Fig. 16. Temperature (K) distribution contours in y and ϕ directions at $\alpha = 1$, $\beta = 1$, $\lambda = 2\,W\,/\,K$ and (a) $\delta = 8\,W\,/\,m^2K$, (b) $\delta = 10\,W\,/\,m^2K$, (c) $\delta = 12\,W\,/\,m^2K$, (d) $\delta = 14\,W\,/\,m^2K$ for case 2.
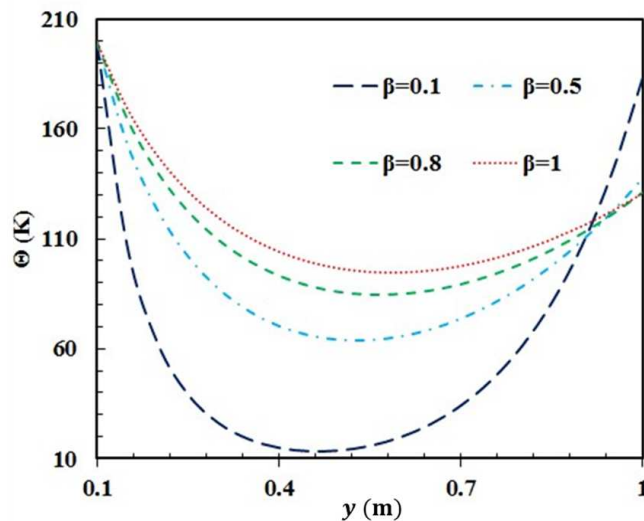
Fig. 17. Temperature distribution in y direction at $\alpha = 1$, $\delta = 10\ W/m^2K$, $\lambda = 3\ W/K$ and (a) $\beta = 0.1$, (b) $\beta = 0.5$, (c) $\beta = 0.8$, (d) $\beta = 1$ for case 2.
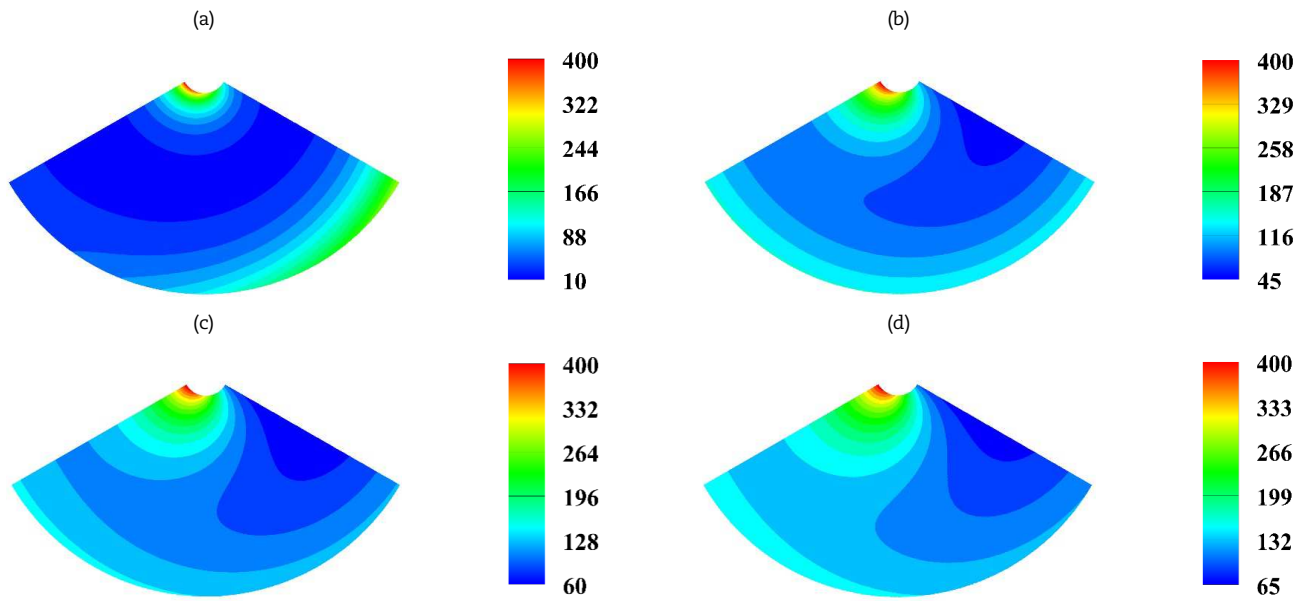
(a)

(b)

(c)

(d)

Fig. 18. Temperature (K) distribution contours in y and ϕ directions at $\alpha = 1$, $\delta = 10\ W/m^2K$, $\lambda = 3\ W/K$ and (a) $\beta = 0.1$, (b) $\beta = 0.5$, (c) $\beta = 0.8$, (d) $\beta = 1$ for case 2.

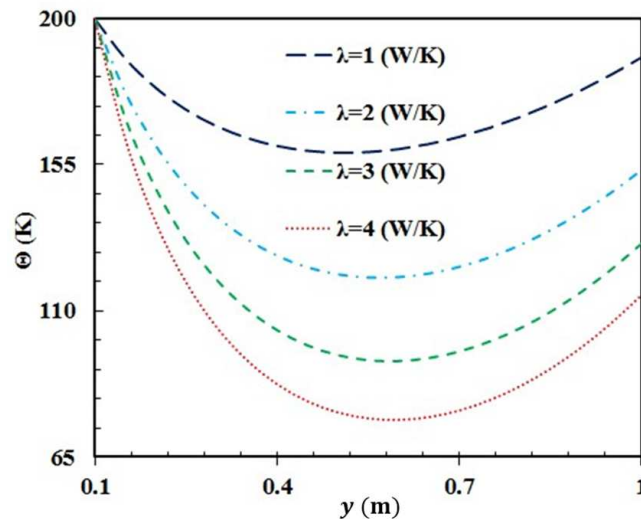**Fig. 19.** Temperature distribution in y direction at $\alpha = 1$, $\delta = 10\ W/m^2K$, $\beta = 1$ and (a) $\lambda = 1\ W/K$, (b) $\lambda = 2\ W/K$, (c) $\lambda = 3\ W/K$, (d) $\lambda = 4\ W/K$ for case 2.

(a)

(b)

Fig. 20. Temperature (K) distribution contours in y and ϕ directions at $\alpha = 1$, $\delta = 10\ W/m^2K$, $\beta = 1$ and (a $\lambda = 1\ W/K$, (b) $\lambda = 2\ W/K$, (c) $\lambda = 3\ W/K$, (d) $\lambda = 4\ W/K$ for case 2.
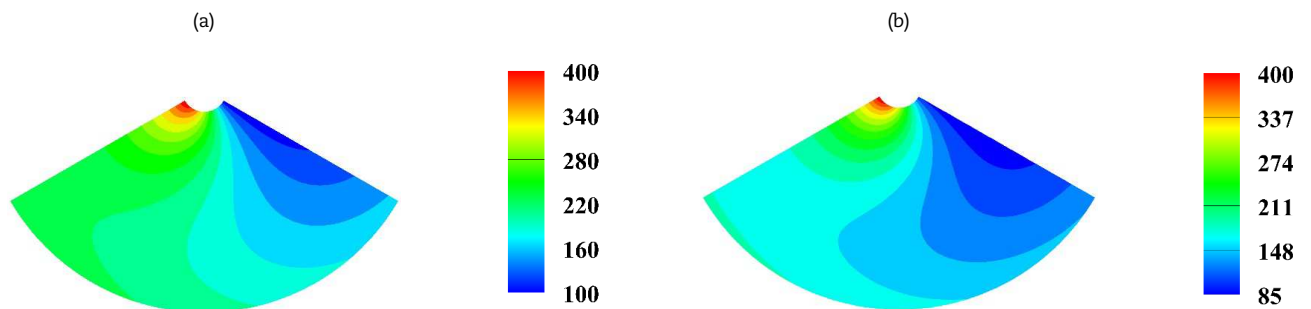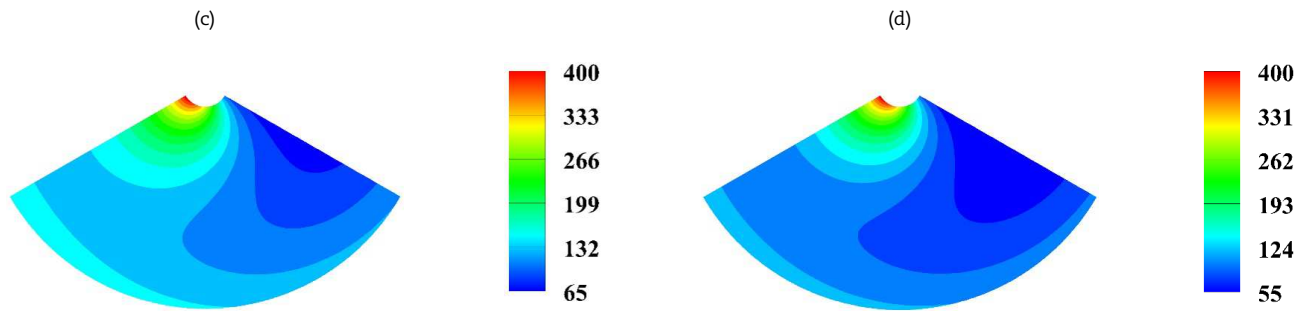
(c)   (d)

Fig. 20. Temperature (K) distribution contours in y and ϕ directions at $\alpha = 1$, $\delta = 10 \ W / m^2 K$, $\beta = 1$ and (a $\lambda = 1 \ W / K$, (b) $\lambda = 2 \ W / K$,

(c) $\lambda = 3 \ W / K$, (d) $\lambda = 4 \ W / K$ for case 2.

5. Conclusion

The study presents an analytical solution for the two-dimensional conduction analysis of functionally graded conical shell with power-law variations. The general thermal conditions are applied to the functionally graded conical body to study a wide range of problems. After properly verifying the results against numerical data, two case examples which are tried to capture the practical conditions and subjected to a number of different boundary conditions are examined in details. The impacts of various parameters like material constant, conductivity ratio, and heat flux on the temperature distribution are studied. The presented analytical solution can help researchers to broaden the scope of research in this field in three ways. 1) The results of the proposed general solution can help in the preconstruction process of conical shells made of functionally graded materials. 2) The results of this analytical solution can be useful for the verification of more complex numerical studies in this field. 3) The current solution which is presented here can help to better understand the mechanisms of heat transfer in FGMs with specific cone geometry.

Author Contributions

A. Amiri Delouei and A. Emamian initiated the project and conducted the analytical study; S. Karimnejad along with the other authors was responsible for writing the manuscript, reviewing the literature and analyzing the obtained results; Y. Li was also responsible for investigating the ongoing problem. The research was conducted through the contribution of all authors. All authors discussed the results, reviewed, and approved the final version of the manuscript.

Acknowledgments

Not applicable.

Conflict of Interest

The authors declared no potential conflicts of interest with respect to the research, authorship, and publication of this article.

Funding

The authors received no financial support for the research, authorship, and publication of this article.

Data Availability Statements

The datasets generated and/or analyzed during the current study are available from the corresponding author on reasonable request.

Nomenclature

A_n, B_n, C_n, D_n	The coefficients of Bessel series	$w_1(\phi), w_2(\phi)$	Arbitrary function of ϕ (W/m²)
A_0, B_0	The constant coefficient zeroth order	y, ϕ	Coordinate system
a	Inner radius (m)	μ, δ	Constant coefficient (W/m²K)
b	Outer radius (m)	υ, ε	Constant coefficient (W/mK)
c	Specific heat capacity (J/Kg K)	β	Conduction coefficients ratio
FGM	Functionally graded material	ρ	Density (Kg/m³)
h	Convective coefficient of heat transfer (W/m²K)	η	Heat flux (W/m²)
k_y, k_ϕ	The heat conductivity coefficients in y and ϕ directions (W/mK)	$\Lambda(y)$	Independent function of y
k_1, k_2	The conduction coefficients in y and ϕ directions (W/mK)	$\Gamma(\phi)$	Independent function of ϕ
R	Radius of cone's annular cross section (m)	α	Material constant coefficient
T	Temperature distribution (K)	Δ_n	Separation constant
$T_{r,\infty}$	The ambient temperature (K)		

References

1.   Tsai S: Introduction to composite materials: Routledge; 2018.

2. Delouei AA, Emamian A, Karimnejad S, Sajjadi H: A closed-form solution for axisymmetric conduction in a finite functionally graded cylinder. *International Communications in Heat and Mass Transfer* 2019, 108: 104280.
3. Loh GH, Pei E, Harrison D, Monzon MD: An overview of functionally graded additive manufacturing. *Additive Manufacturing* 2018, 23: 34-44.
4. Chen M, Jin G, Ma X, Zhang Y, Ye T, Liu Z: Vibration analysis for sector cylindrical shells with bi-directional functionally graded materials and elastically restrained edges. *Composites Part B: Engineering* 2018, 153: 346-363.
5. Jain PK, Singh S: An exact analytical solution for two-dimensional, unsteady, multilayer heat conduction in spherical coordinates. *International Journal of Heat and Mass Transfer* 2010, 53(9-10): 2133-2142.
6. Udupa G, Rao SS, Gangadharan K: Functionally graded composite materials: an overview. *Procedia Materials Science* 2014, 5: 1291-1299.
7. Bayat M, Alarifi IM, Khalili AA, El-Bagory TM, Nguyen HM, Asadi A: Thermo-mechanical contact problems and elastic behaviour of single and double sides functionally graded brake disks with temperature-dependent material properties. *Scientific reports* 2019, 9(1): 1-16.
8. Haghighi MG, Eghtesad M, Malekzadeh P, Necsulescu D: Two-dimensional inverse heat transfer analysis of functionally graded materials in estimating time-dependent surface heat flux. *Numerical Heat Transfer, Part A: Applications* 2008, 54(7): 744-762.
9. Birman V: Functionally graded materials and structures. *Encyclopedia of Thermal Stresses* 2014: 1858-1865.
10. Hetnarski RB: Encyclopedia of thermal stresses: Springer Netherlands; 2014.
11. Clyne T, Hull D: An introduction to composite materials: Cambridge University Press; 2019.
12. Li M, Chen C, Chu C, Young D: Transient 3D heat conduction in functionally graded materials by the method of fundamental solutions. *Engineering Analysis with Boundary Elements* 2014, 45: 62-67.
13. Shen H-S: Functionally graded materials: nonlinear analysis of plates and shells: CRC Press; 2016.
14. Delouei AA, Emamian A, Karimnejad S, Sajjadi H, Jing D: Two-dimensional temperature distribution in FGM sectors with the power-law variation in radial and circumferential directions. *Journal of Thermal Analysis and Calorimetry* 2020: 1-11.
15. Udupa G, Rao S, Gangadharan K: Functionally Graded Composite Materials: An Overview, Procedia Materials Science, 5 (2014) 1291-1299. In: *International Conference on Advances in Manufacturing and Materials Engineering, ICAMME:* 2014.
16. Yang Y, Munz D: Stress analysis in a two materials joint with a functionally graded material. In: *Functionally Graded Materials 1996.* Elsevier; 1997: 41-46.
17. Harris JL, Vendely MJ, Eckert CE, Shelton IV FE: Composite adjunct materials for delivering medicants. In.: Google Patents; 2019.
18. Kayhani M, Norouzi M, Delouei AA: A general analytical solution for heat conduction in cylindrical multilayer composite laminates. *International Journal of Thermal Sciences* 2012, 52: 73-82.
19. Delouei AA, Kayhani M, Norouzi M: Exact analytical solution of unsteady axi-symmetric conductive heat transfer in cylindrical orthotropic composite laminates. *International Journal of Heat and Mass Transfer* 2012, 55(15-16): 4427-4436.
20. Delouei AA, Norouzi M: Exact analytical solution for unsteady heat conduction in fiber-reinforced spherical composites under the general boundary conditions. *Journal of Heat Transfer* 2015, 137(10): 101701.
21. Kayhani M, Delooei AA: An exact solution of axi-symmetric conductive heat transfer in cylindrical composite laminate under the general boundary condition. 2010.
22. Norouzi M, Delouei AA, Seilsepour M: A general exact solution for heat conduction in multilayer spherical composite laminates. *Composite Structures* 2013, 106: 288-295.
23. Yang B, Liu S: Closed-form analytical solutions of transient heat conduction in hollow composite cylinders with any number of layers. *International Journal of Heat and Mass Transfer* 2017, 108: 907-917.
24. Li M, Lai AC: Analytical solution to heat conduction in finite hollow composite cylinders with a general boundary condition. *International Journal of Heat and Mass Transfer* 2013, 60: 549-556.
25. Gupta A, Talha M: Recent development in modeling and analysis of functionally graded materials and structures. *Progress in Aerospace Sciences* 2015, 79: 1-14.
26. Suresh S, Mortensen A: Fundamentals of functionally graded materials: The Institut of Materials; 1998.
27. Swaminathan K, Naveenkumar D, Zenkour A, Carrera E: Stress, vibration and buckling analyses of FGM plates—A state-of-the-art review. *Composite Structures* 2015, 120: 10-31.
28. Sofiyev A: Thermoelastic stability of functionally graded truncated conical shells. *Composite Structures* 2007, 77(1): 56-65.
29. Shahmardan MM, Norouzi M, Kayhani MH, Delouei AA: An exact analytical solution for convective heat transfer in rectangular ducts. *Journal of Zhejiang University SCIENCE A* 2012, 13(10): 768-781.
30. Wang H, Cao L, Qin Q-H: Hybrid graded element model for nonlinear functionally graded materials. *Mechanics of Advanced Materials and Structures* 2012, 19(8): 590-602.
31. Sutradhar A, Paulino GH: The simple boundary element method for transient heat conduction in functionally graded materials. *Computer Methods in Applied Mechanics and Engineering* 2004, 193(42-44): 4511-4539.
32. Norouzi M, Emamian A, Davoodi M: An analytical and experimental study on dynamics of a circulating Boger drop translating through Newtonian fluids at inertia regime. *Journal of Non-Newtonian Fluid Mechanics* 2019, 267: 1-13.
33. Lu X, Tervola P, Viljanen M: Transient analytical solution to heat conduction in composite circular cylinder. *International Journal of Heat and Mass Transfer* 2006, 49(1-2): 341-348.
34. Lin R-L: Explicit full field analytic solutions for two-dimensional heat conduction problems with finite dimensions. *International Journal of Heat and Mass Transfer* 2010, 53(9-10): 1882-1892.
35. Swaminathan K, Sangeetha D: Thermal analysis of FGM plates–A critical review of various modeling techniques and solution methods. *Composite Structures* 2017, 160: 43-60.
36. Dai H-L, Rao Y-N, Dai T: A review of recent researches on FGM cylindrical structures under coupled physical interactions, 2000–2015. *Composite Structures* 2016, 152: 199-225.
37. Malekzadeh P, Golbahar Haghighi M, Heydarpour Y: Heat transfer analysis of functionally graded hollow cylinders subjected to an axisymmetric moving boundary heat flux. *Numerical Heat Transfer, Part A: Applications* 2012, 61(8): 614-632.
38. Malekzadeh P, Heydarpour Y: Response of functionally graded cylindrical shells under moving thermo-mechanical loads. *Thin-walled structures* 2012, 58: 51-66.
39. Rahideh H, Malekzadeh P, Haghighi MG: Heat conduction analysis of multi-layered FGMs considering the finite heat wave speed. *Energy Conversion and Management* 2012, 55: 14-19.
40. Delouei AA, Emamian A, Karimnejad S, Sajjadi H, Tarokh A: On 2D asymmetric heat conduction in functionally graded cylindrical segments: A general exact solution. *International Journal of Heat and Mass Transfer* 2019, 143: 118515.
41. Delouei AA, Emamian A, Karimnejad S, Sajjadi H, Jing D: Asymmetric Conduction in an Infinite Functionally Graded Cylinder: Two-Dimensional Exact Analytical Solution Under General Boundary Conditions. *Journal of Heat Transfer* 2020, 142(4).
42. Delouei AA, Emamian A, Karimnejad S, Sajjadi H, Jing D: Two-dimensional analytical solution for temperature distribution in FG hollow spheres: General thermal boundary conditions. *International Communications in Heat and Mass Transfer* 2020, 113: 104531.
43. Thai H-T, Kim S-E: A review of theories for the modeling and analysis of functionally graded plates and shells. *Composite Structures* 2015, 128: 70-86.
44. Hosseini SM, Akhlaghi M, Shakeri M: Transient heat conduction in functionally graded thick hollow cylinders by analytical method. *Heat and Mass Transfer* 2007, 43(7): 669-675.
45. Eslami M, Babaei M, Poultangari R: Thermal and mechanical stresses in a functionally graded thick sphere. *International Journal of Pressure Vessels and Piping* 2005, 82(7): 522-527.
46. Sofiyev A: Thermoelastic stability of freely supported functionally graded conical shells within the shear deformation theory. *Composite Structures* 2016, 152: 74-84.
47. Sofiyev A, Zerin Z, Kuruoglu N: Thermoelastic buckling of FGM conical shells under non-linear temperature rise in the framework of the shear deformation theory. *Composites Part B: Engineering* 2017, 108: 279-290.
48. Bhangale RK, Ganesan N, Padmanabhan C: Linear thermoelastic buckling and free vibration behavior of functionally graded truncated conical shells. *Journal of Sound and Vibration* 2006, 292(1-2): 341-371.
49. Sofiyev A: The non-linear vibration of FGM truncated conical shells. *Composite Structures* 2012, 94(7): 2237-2245.

50. Kiani Y, Dimitri R, Tornabene F: Free vibration study of composite conical panels reinforced with FG-CNTs. *Engineering Structures* 2018, 172: 472-482.

51. Daneshjou K, Bakhtiari M, Alibakhshi R, Fakoor M: Transient thermal analysis in 2D orthotropic FG hollow cylinder with heat source. *International Journal of Heat and Mass Transfer* 2015, 89: 977-984.

52. Sofiyev A: Large amplitude vibration of FGM orthotropic cylindrical shells interacting with the nonlinear Winkler elastic foundation. *Composites Part B: Engineering* 2016, 98: 141-150.

53. Nikbakht S, Kamarian S, Shakeri M: A review on optimization of composite structures Part II: Functionally graded materials. *Composite Structures* 2019.

54. Norouzi M, Rahmani H: On exact solutions for anisotropic heat conduction in composite conical shells. *International Journal of Thermal Sciences* 2015, 94: 110-125.

55. Crawford M, Kays W: Convective heat and mass transfer. *McGraw-FEE* 1993.

ORCID iD

Amin Amiri Delouei https://orcid.org/0000-0001-7414-4195
Amin Emamian https://orcid.org/0000-0002-7568-0691
Sajjad Karimnejad https://orcid.org/0000-0002-2691-181X
Yueming Li https://orcid.org/0000-0002-4787-8369

Publisher's Note Shahid Chamran University of Ahvaz remains neutral with regard to jurisdictional claims in published maps and institutional affiliations.